THE JOURNAL OF PHYSICAL CHEMISTRY B

Article

pubs.acs.org/JPCB

Computation of Standard Binding Free Energies of Polar and Charged Ligands to the Glutamate Receptor GluA2

Germano Heinzelmann,[†] Po-Chia Chen,[‡] and Serdar Kuyucak[†,*]

[†]School of Physics, University of Sydney, New South Wales 2006, Australia

[‡]Computational Molecular Biophysics Group, Department of Molecular Structural Biology, Georg-August-University, 37073 Göttingen, Germany

ABSTRACT: Accurate calculation of the binding affinity of small molecules to proteins has the potential to become an important tool in rational drug design. In this study, we use the free energy perturbation (FEP) method with restraints to calculate the standard binding free energy of five ligands (ACPA, AMPA, CNQX, DNQX, and glutamate) to the glutamate receptor GluA2, which plays an essential role in synaptic transmission. To deal with the convergence problem in FEP calculations with charged ligands, we use a protocol where the ligand is coupled in the binding site while it is decoupled in bulk solution simultaneously. The contributions from the conformational, rotational, and translational entropies to the standard binding free energy are determined by applying/releasing respective restraints to the ligand in bulk/binding site. We also employ the confine-and-release approach, which helps to resolve convergence problems in FEP calculations. Our results are in good agreement with the experimental values for all five ligands, including the charged ones which are often problematic in FEP calculations. We also analyze the different contributions to the binding free energy of each ligand to GluA2 and discuss the nature of these interactions.

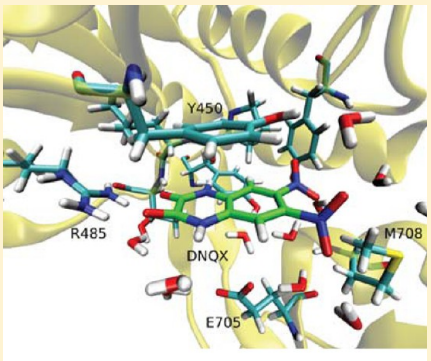

INTRODUCTION

The mechanism of action of many pharmaceutical drugs relies on binding of small molecules to receptor sites with high affinity and specificity.[1,2] If we can find efficient ways to calculate the protein−ligand binding affinities accurately, computational methods could become a powerful tool in the discovery and optimization of lead molecules.[3] To achieve that goal, one needs both a well-parametrized force field and a suitable method for calculating binding free energies. Software packages such as Antechamber in AMBER[4] and CGenFF in CHARMM[5,6] provide missing force-field parameters for drug-like molecules so that they can be incorporated in simulations of biomolecules. These parameters can be further optimized by performing quantum mechanical calculations using programs such as Gaussian 09.[7] Binding free energies of ligands can be calculated in a number of ways, and generally, greater accuracy of the results comes at a larger computational cost. Simple empirical scoring functions can sieve through millions of compounds, which may be desirable in an industrial environment.[8] However, these simplifications often compromise the accuracy of the predictions made.[9] At the other end of the spectrum, we have the free energy perturbation (FEP) and potential of mean force (PMF) methods that use all-atom molecular dynamics (MD) simulations.[10−17] They provide the most accurate approach for the prediction of ligand binding affinities, but they are also very time-consuming and computationally costly. Nevertheless, thanks to the consistent, rapid increase in computing power and improvements in computational methods, these MD methods are fast becoming viable alternatives for lead selection.

Depending on the ligand−receptor system, the FEP or the PMF method may be more appropriate for the calculation of binding affinities. An important consideration in this regard is the size and charge state of the ligand, which determine its hydration energy. For small, neutral molecules, the hydration energy can be calculated accurately using the FEP method.[18,19] Hence FEP has become the standard method for such molecules.[20−27] Here the ligand interactions are decoupled from the rest of the system in both the binding site and bulk solvent, and the free energy of binding is obtained from the difference of these transformations. The standard binding free energies—needed for comparison of the results to experimental binding constants—are obtained by including entropy terms that take into account the loss of translational, rotational, and conformational freedoms of the ligand upon binding.[28−34]

For large and especially charged molecules, the FEP method has rarely been used due to convergence problems, and therefore, the PMF method has been the method of choice.[35−43] The PMF is determined along one or more reaction coordinates of the ligand with respect to the receptor, and the free energy of binding is obtained by integrating the PMF along these coordinates. Even though in PMF calculations the ligand does not need a clear pathway to the binding site,[34] these calculations become very difficult for ligands that are buried inside proteins. Such a situation occurs in the closed state of ionotropic glutamate

Received: December 13, 2013
Revised: January 30, 2014
Published: January 31, 2014

dx.doi.org/10.1021/jp412195m | J. Phys. Chem. B 2014, 118, 1813−1824

receptors, where the ligand is partially isolated from the solvent. One way to deal with this problem is to create an open state so as to establish a clear pathway for the ligand. This method was recently applied to binding of neurotransmitters to the ionotropic glutamate receptor GluA2.[44] While good results were obtained for the binding free energies of several ligands, in general, it would be desirable to perform the free energy calculations using directly the crystal structures. This is feasible using the FEP method, where only the end points are needed in the calculations. Therefore, it is worthwhile to examine the convergence problem in FEP and see if it can be resolved using a different protocol than the one commonly used. In most FEP calculations, the decouplings of the ligand from the binding site and bulk solution are performed in separate simulations. By increasing the system size slightly, it is possible to perform both transformations simultaneously, that is, coupling the ligand in the binding site while decoupling it in bulk at the same time. For charged ligands, this approach also solves the neutrality problem so that one does not need to annihilate ions together with the ligand in order to keep the system neutral during the FEP calculations[45] or include correction terms for the inserted charges.[46] This method was recently used in FEP calculations of aspartate binding to the transporter protein Glt_{Ph},[47,48] and free energy change due to a charge mutation in a bound toxin[49] and was shown to yield consistent results with experiments.

The aim of this work is to perform extensive FEP calculations using the above protocol to determine the binding free energies of five ligands (ACPA, AMPA, CNQX, DNQX, and glutamate) to the S1S2 ligand binding domain (LBD) of GluA2. Glutamate is the predominant excitatory neurotransmitter in the brain, and ionotropic glutamate receptors are essential for the fast synaptic transmission between nerve cells.[50] They work by coupling the binding of a ligand to the opening of an ion channel, which allows flow of cations through the membrane and transmission of a nerve impulse. This coupling is related to the closure of the clamshell-shaped LBD in the presence of agonists such as glutamate and AMPA. Antagonists such as CNQX and DNQX, on the other hand, bind to GluA2 but do not allow the closure of the LBD, thereby blocking receptor activation. From a biomedical point of view, it has been shown that malfunctioning of the GluA2 receptors is implicated in a range of diseases, including stroke, depression, and Parkinson's disease.[51,52] Accurate calculation of the free energies involved in ligand binding and the closure of the LBD will help to understand the mechanism of synaptic transmission,[44] which will facilitate finding treatments for such diseases.

There are several other reasons for choosing GluA2 in this study. First, there are high-resolution crystal structures of GluA2 in the apo state and in complex with all of the ligands tested,[53−56] so that any conformational changes in GluA2 due to their presence can be easily identified. Next, the experimental binding free energies of these ligands are available in the literature,[53−56] so we can test the accuracy of our calculations. Finally, there are computational studies that use umbrella sampling[44] and metadynamics[57] to obtain the ligand affinities, which can be directly compared to our FEP results. In umbrella sampling simulations,[44] ∼13 ns was used to calculate the binding affinity of each ligand from a one-dimensional PMF, plus ∼40 ns to calculate the conformational PMF of the receptor in each case. Much longer simulation times were used in ref 57 with 0.5 μs of metadynamics simulations for the opening of the receptor LBD and 13.5 μs for calculating the binding affinity of each ligand to the open state.

In the following sections, we first discuss the theoretical background and the methodology used in our calculations. We then present the results and compare the binding free energies obtained using the FEP method to the experimental/computational values available in the literature. For all five ligands considered, the FEP results are found to be in good agreement with the ones obtained by experiment and through umbrella sampling simulations.

THEORY AND METHODS

Standard Binding Free Energy. The standard binding free energy for binding of a ligand to a receptor is defined from the equilibrium constant K_b as

$$\Delta G_b^0 = -k_B T \ln(C^0 K_b) \quad (1)$$

where C^0 is the standard concentration of 1 mol/L = 1/(1661 Å^3). For computational convenience, ΔG_b^0 can be decomposed as follows[11−13]

$$\Delta G_b^0 = \Delta\Delta G_{cf} + \Delta\Delta G_{rot} + \Delta\Delta G_{tr}^0 + \Delta\Delta G_{int} + \Delta G_{close} \quad (2)$$

where the first three terms represent the free energy contributions due to the changes in the conformational, rotational, and translational entropies of the ligand upon binding and the fourth term gives the interaction free energy difference for translocating the ligand from the bulk to the binding site. The last term in eq 2 represents the free energy change due to conformational rearrangements in the receptor upon ligand binding such as the closure of the glutamate receptor. Straightforward calculation of the interaction energy term without any restraints on the ligand runs into a convergence problem because it is difficult to sample all possible states of the ligand in both the binding site and bulk solvent. This problem is resolved in the double decoupling method (DDM),[11−13] where restraints are imposed on the ligand while its interactions with the solvent/receptor are decoupled/coupled. The contributions from these restraints are taken into account separately by means of simulations or analytical methods.

The thermodynamic cycle we use in the FEP calculations is illustrated in Figure 1, which describes the binding of a ligand to

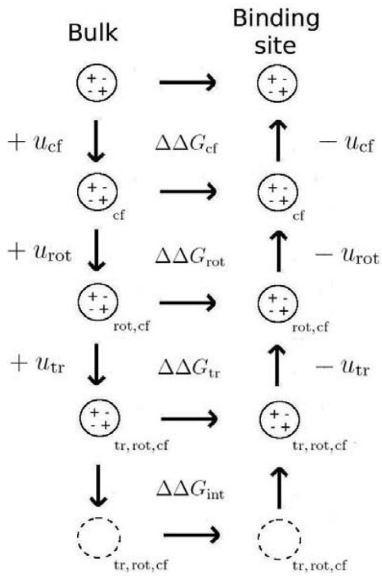

Figure 1. Thermodynamic cycle used in the FEP calculations, where the restraints are applied on the ligand in bulk solution and released while it is at the binding site.

dx.doi.org/10.1021/jp412195m | J. Phys. Chem. B 2014, 118, 1813−1824

the receptor site. The ligand is restrained in bulk using conformational, rotational, and translational potentials denoted by u_c, u_r, and u_t, respectively. The restrained ligand is then translocated from bulk to the binding site, followed by removal of the restraints in reverse order. In what follows, we first describe the free energy changes associated with the application/release of the restraints followed by the interaction energy.

Conformational Free Energy. Conformational restraining of a ligand in bulk/binding site is achieved using the harmonic potential

$$u_c = \frac{k_c}{2n}\sum_{i=1}^{n}(x_i - x_{0i})^2 \tag{3}$$

with k_c = 50 (kcal/mol)/Å^2. Here $\{x_i, i = 1, ..., n\}$ give the current positions of the ligand atoms after its position and orientation have been aligned with the reference state described by $\{x_{0i}, i = 1, ..., n\}$. The reference state is chosen as the average conformation of the fully interacting ligand in the bulk/binding site when no restraints are applied. The conformational free energy difference for applying the restraint in bulk and releasing it in the binding site is given by (see Figure 1)

$$\Delta\Delta G_{cf} = \Delta G_{cf}^{bulk} - \Delta G_{cf}^{site} \tag{4}$$

The bulk/site contributions to ΔG_{cf} are determined in separate FEP calculations where k_c is relaxed from 50 (kcal/mol)/Å^2 to 0 in ten steps given by {50, 30, 15, 8, 4, 2, 1, 0.5, 0.2, 0.1, 0}. Each FEP window is equilibrated for 300 ps followed by 800 ps of production data collection, and the free energy is obtained via numerical integration of the window values.

Rotational and Translational Free Energies. In recent calculations of the standard free energy of ligands, the translational and rotational freedoms of the ligand are restrained relative to the protein using anchoring atoms in the ligand and the protein.[23−27] This can be done in a number of ways, but it is essential that these anchors are chosen properly.[58] Here we use instead the body restraint algorithm,[29] where the absolute coordinates are employed for both the position and orientation of the ligand, even though these quantities must be determined relative to the protein in order to obtain accurate results. We circumvent this problem by strongly restraining the orientation and the position of the center of mass (COM) of our receptor, such that these restraints are much larger than the restraints applied on the ligand. We stress that the strong restraints applied on the receptor affect only its position of the COM and overall orientation but not its internal degrees of freedom.

The orientational restraints are applied using the quaternion formalism: for a given ligand orientation $\mathbf{q}$ and its average orientation $\mathbf{q}_0$, the restraining potential is given by $u_r = (k_r/2)\Omega^2$, where $\Omega = \cos^{-1}(\mathbf{q}\cdot\mathbf{q}_0)$ and k_r = 300 (kcal/mol)/rad^2 is employed. Similarly, a harmonic potential of the form $u_t = (k_t/2)(\mathbf{r} - \mathbf{r}_0)^2$ is used to restrain the COM of the ligand in the binding site with k_t = 10 (kcal/mol)/Å^2. The average orientation $\mathbf{q}_0$ and the average position $\mathbf{r}_0$ are determined from restraint-free MD simulations of the ligand in the binding site. The magnitude of the spring constants k_r and k_t are chosen according to the fluctuations of the associated coordinates, namely, $k_t \sim 3k_BT/\langle(\mathbf{r} - \mathbf{r}_0)^2\rangle$ and $k_r \sim 3k_BT/\langle\Omega^2\rangle$. The force constants applied to the position and orientation of the protein are about a hundred times larger than the ones applied on the ligand. This ensures that the protein can be considered fixed in space compared to the fluctuations of the ligand, and hence we can safely use the absolute coordinates of the ligand in the calculations.

The free energy differences associated with the application/release of the rotational and translational restraints in bulk/binding site are given by

$$\Delta\Delta G_{rot} = \Delta G_{rot}^{bulk} - \Delta G_{rot}^{site} \tag{5}$$

$$\Delta\Delta G_{tr}^{0} = \Delta G_{tr}^{bulk} - \Delta G_{tr}^{site} \tag{6}$$

The binding site contributions to both terms are determined by performing FEP calculations similar to those of the conformational case. For ΔG_{rot}^{site}, k_r is relaxed from 300 (kcal/mol)/rad^2 to 0 in eleven steps given by {300, 200, 150, 80, 50, 30, 15, 8, 4, 2, 1, 0}. Similarly for ΔG_{tr}^{site}, k_t is relaxed from 10 (kcal/mol)/Å^2 to 0 in eight steps given by {10, 8, 5, 2, 1, 0.5, 0.2, 0.1, 0}. In both FEP calculations, each window is equilibrated for 300 ps followed by 800 ps of data collection. The bulk contributions can be determined analytically using the rigid-rotor approximation, which works well for conformationally restrained ligands[24]

$$\Delta G_{rot}^{bulk} = -k_BT\ln\left[\frac{1}{8\pi^2}\int e^{-u_r(\phi_1,\phi_2,\phi_3)/k_BT}\,d\phi_1\,d\phi_2\,d\phi_3\right] = -k_BT\ln\left[\frac{1}{8\pi^2}\left(\frac{2\pi k_BT}{k_r'}\right)^{3/2}\right] \tag{7}$$

$$\Delta G_{tr}^{bulk} = -k_BT\ln\left[\frac{1}{V_0}\int e^{-u_t(\mathbf{r})/k_BT}\,d^3r\right] = -k_BT\ln\left[\frac{1}{V_0}\left(\frac{2\pi k_BT}{k_t}\right)^{3/2}\right] \tag{8}$$

where V_0 = 1661 Å^3 is the reference volume for the standard concentration. In obtaining eq 7, we have converted the quaternion representation to the three axes of rotation assuming that they are not coupled, which is valid for small rotations. Therefore k_r' in eq 7 represents the spring constant applied to the three rotation axes.

It is of interest to compare the rotational and translational free energy differences obtained from the application of restraints with the corresponding ones obtained directly from the rotational and translational entropy differences for binding of a free ligand to a receptor site[28−32]

$$\Delta\Delta G_{rot\text{-}ent} = -k_BT\ln\left[\frac{(2\pi e)^{3/2}\sigma_{\phi_1}\sigma_{\phi_2}\sigma_{\phi_3}}{8\pi^2}\right] \tag{9}$$

$$\Delta\Delta G_{tr\text{-}ent}^{0} = -k_BT\ln\left[\frac{(2\pi e)^{3/2}\sigma_x\sigma_y\sigma_z}{V_0}\right] \tag{10}$$

Here σ_x, σ_y, and σ_z are the principal root-mean-square (rms) fluctuations of the COM of the ligand in the binding site, and σ_{ϕ_1}, σ_{ϕ_2}, and σ_{ϕ_3}, are the principal rotational rms fluctuations of the ligand calculated using the quaternion representation.[32] The various σ values are calculated by performing 6 ns of MD simulations of the unrestrained ligand in the binding site and diagonalizing the translational and rotational covariance matrices obtained from the trajectory data.[31,32] The MD simulations show that the six degrees of freedom associated with the positions and orientations of the ligands in the binding site are well-described by normal distributions so that the entropic contributions to the

dx.doi.org/10.1021/jp412195m | J. Phys. Chem. B 2014, 118, 1813−1824

binding free energy can be determined accurately using eqs 9 and 10. Although eqs 5 and 6 are formally different from eqs 9 and 10, we will show in Results and Discussion that they lead to very similar results when the restraining potentials are chosen appropriately.

Interaction Free Energy. The free energy of translocation, that is, decoupling the restrained ligand in bulk and coupling it in the binding site, is given by

$$\Delta\Delta G_{\text{int}} = \Delta G_{\text{int}}^{\text{site}} - \Delta G_{\text{int}}^{\text{bulk}} \tag{11}$$

Here we perform the binding site and bulk calculations simultaneously and in the same system, which helps to maintain the neutrality of the system for charged ligands.[47,48] Performing these calculations separately could lead to substantial errors due to the large solvation free energies associated with charged ligands.[35] In the present approach, the electrostatic part of the alchemical transformation can be seen as a transfer of charge between two regions of the same system. This reduces the errors arising from the large solvation energies of charged ligands as well as potential artifacts from use of the periodic boundary conditions.

The free energy of translocation in eq 11 is calculated using the FEP and thermodynamic integration (TI) methods.[15] In both methods, one introduces a hybrid Hamiltonian $H(\lambda) = (1 - \lambda)H_0 + \lambda H_1$, where H_0 represents the Hamiltonian for the initial state and H_1 for the final state of the system. In the FEP method, the interval between $\lambda = 0$ and 1 is divided into n subintervals with $\{\lambda_i, i = 1, ..., n - 1\}$, and for each subinterval the free energy difference is calculated from the ensemble average

$$\Delta G_i = -k_{\text{B}}T \ln\langle \exp[-(H(\lambda_{i+1}) - H(\lambda_i))/k_{\text{B}}T]\rangle_{\lambda_i} \tag{12}$$

The free energy of translocation is then obtained from the sum, $\Delta G_{\text{int}} = \Sigma_i \Delta G_i$. In the TI method, the ensemble average of the derivative, $\partial H(\lambda)/\partial\lambda$, is obtained at several λ values, and the free energy of translocation is calculated from the integral

$$\Delta G_{\text{int}} = \int_0^1 \left\langle \frac{\partial H(\lambda)}{\partial \lambda} \right\rangle_\lambda \mathrm{d}\lambda \tag{13}$$

This integral is evaluated using a seven-point or nine-point Gaussian quadrature, which has been shown to provide a good method for free energy calculations involving translocation of charged ligands.[47,48] In order to improve convergence and prevent instabilities in the FEP and TI calculations, decoupling/coupling of the ligand in bulk/site is performed in two stages by separating the Coulomb and Lennard-Jones (LJ) interactions

$$\Delta\Delta G_{\text{int}} = \Delta\Delta G_{\text{elec}} + \Delta\Delta G_{\text{LJ}} \tag{14}$$

In the calculations, first the electrostatic interactions of the ligand are switched off/on in bulk/site followed by decoupling/coupling of the LJ interactions in bulk/site. We also use a soft-core potential for the LJ interactions to avoid problems at the end-points of the simulations.[59]

In the FEP calculations, it is important to choose the number of windows such that the ΔG_i value in each window is not much larger than 1.5 kT.[15] For the electrostatic terms in CNQX and DNQX, 66 windows are found to be sufficient while for ACPA, AMPA, and glutamate—which carry charged groups—100 windows are required in order to obtain good convergence. Each window is equilibrated for 80 ps followed by a 120 ps production run. In the case of the LJ interactions, 60 λ values are used for all ligands with smaller intervals close to the end-points. Each window is equilibrated for 80 ps followed by 80 ps of data collection. The windows for the TI calculations are adapted from those created during the FEP simulations. For the electrostatic terms, seven windows are used with 300 ps of equilibration and either 1 ns (CNQX and DNQX) or 1.5 ns (ACPA, AMPA, and glutamate) of data collection. For the LJ terms, seven windows are used for CNQX and DNQX and nine windows for ACPA, AMPA, and glutamate. In this case each window is equilibrated for 200 ps followed by 1 ns of production. The statistical errors in the TI calculations are estimated by performing block data analysis, using blocks of 100 ps. This does not take into account any systematic errors arising from the force field used or the asymmetry between the insertion and deletion of particles.[60] An estimate for the latter can be obtained from hysteresis between the forward and backward calculations.

To assess the convergence of the FEP and TI calculations, it is important to perform both the forward and the backward transformations and check for consistency between the two results. A large hysteresis may be an indication of an energy barrier that cannot be crossed within the time scales of individual windows, and the results will not be reliable. In such situations, TI may provide a better option than FEP due to longer sampling of a smaller number of windows. Here we look for agreement between the forward and backward transformations in both FEP and TI calculations, and use it as evidence that our calculations are properly converged. The interaction binding free energy is determined from the average of the forward and the negative of the backward transformation results. In many studies, the Bennett acceptance ratio method[61,62] is used to obtain the optimal value of ΔG_i. This method uses an ensemble of forward and backward transformations at each window, in order to get the maximum likelihood estimator for the free energy difference. Here we perform the whole transformation in both directions, and the σ values are based only on the TI calculations. Nevertheless, we can still obtain an estimate of the boundary values for the FEP calculations from the forward and backward results. According to the Gibbs–Bogoliubov inequality,[61] the optimal value of the free energy difference lies between the values of the forward and the backward calculations. The values we obtain using TI are mostly within the range specified by FEP, which indicates consistency between the FEP and TI methods.

Confine and Release. Conformational changes in a protein that take place upon binding/unbinding of a ligand can sometimes affect convergence and prevent obtaining accurate results using FEP. This has been the case in the FEP calculations of the electrostatic terms for AMPA and glutamate, where a large hysteresis is observed between the forward and backward transformations. The problem is traced to the formation of a salt bridge between the ligand's α-amino group and the E705 side chain in GluA2. To resolve this problem we use the confine-and-release method,[63] which is a FEP/PMF hybrid—FEP is used to calculate the binding free energy of the ligand to the confined protein, and the free energy of confinement is obtained from the PMF of the confining coordinate. The interaction free energy can be written as

$$\Delta\Delta G_{\text{int}} = \Delta\Delta G_{\text{int,C}} + \Delta G_{\text{con}} + \Delta G_{\text{rel}} \tag{15}$$

where $\Delta\Delta G_{\text{int,C}}$ represents the free energy of translocation of the restrained ligand to the confined protein and ΔG_{con} and ΔG_{rel} are respectively the free energies of confining the protein in the apo state and removing these restraints in the bound state. These are calculated from

$$\Delta G_{\text{con}} = -\Delta G_{\text{rel}} = -k_{\text{B}}T \ln\left(\frac{\sum_{i\in S_\alpha} \mathrm{e}^{-F_i/k_{\text{B}}T}}{\sum_{\text{all}} \mathrm{e}^{-F_i/k_{\text{B}}T}}\right) \tag{16}$$

dx.doi.org/10.1021/jp412195m | J. Phys. Chem. B 2014, 118, 1813–1824

Table 1. Standard Binding Free Energies of the Five Ligands Considered in This Study[a]

	CNQX	DNQX	ACPA	Glu	AMPA
$\Delta\Delta G_{cf}$	0.2	0.6	0.9	0.3	0.7
$\Delta\Delta G_{rot}$	4.4	3.2*	4.5	3.9	4.6
$\Delta\Delta G^0_{tr}$	3.8	3.6	4.1	3.8	4.0
ΔG_{con}				0.5	1.1
ΔG_{rel}				−2.3	−7.9
$\Delta\Delta G_{elec}$	−7.3 ± 0.6	−6.9 ± 0.6	−10.6 ± 1.1	−5.5 ± 1.6	−4.8 ± 1.1
$\Delta\Delta G_{LJ}$	−7.0 ± 1.3	−7.8 ± 1.4	−0.8 ± 0.7	0.9 ± 0.9	−1.0 ± 1.3
$\Delta G^0_b - \Delta G_{close}$	−5.9 ± 1.4	−7.3 ± 1.5	−1.9 ± 1.3	1.6 ± 1.8	−3.3 ± 1.7
ΔG_{close}[44]	−1.7	−1.6	−10.4	−10.1	−8.3
ΔG^0_b	−7.6 ± 1.4	−8.9 ± 1.5	−12.3 ± 1.3	−8.5 ± 1.8	−11.6 ± 1.7
ΔG^0_b (US)[44]	−7.7	−7.9	−11.2	−9.1	−10.1
ΔG^0_b (exp)	−8.5[53]	−8.2[54]	−10.6[55]	−8.4[54]	−10.8[55]

[a]The free energy changes due to conformational, rotational, and translational restraints are given in rows 1, 2, and 3, respectively. The confine-and-release results (eq 16) for glutamate and AMPA are given in rows 4 and 5. The electrostatic and LJ contributions to the interaction free energy differences obtained from TI calculations are listed in rows 6 and 7. The binding free energies of the ligands to the open state of the receptor (sum of rows 1−7) are given in row 8. The standard binding free energies in row 10 are obtained by adding the free energies of closure from ref 44 (row 9) to the open state results in row 8. The standard binding free energies obtained in this work (row 10) are compared to those determined from umbrella sampling (row 11) and experiments (row 12). The rotational free energies of DNQX (marked with a *) include a factor of $-k_BT \ln(2) = -0.41$, due to the two-fold symmetry of this ligand. All energies are in kcal/mol.

where S_α are the bins in the confined region, and F_i are the free energies for each bin in the apo states for ΔG_{con} and the bound states for ΔG_{rel}. These are computed by performing umbrella sampling simulations for the chosen confinement coordinate(s) and constructing the associated PMF using the weighted histogram analysis method.[64]

The confine-and-release approach can be related to the method used in refs 34 and 35, where the conformation of the ligand is confined and then released in the unbound and bound states. Here we are interested only in the conformational changes in the receptor that are related to the salt bridge in question. Using an overall conformational ensemble as in refs 34 and 35 would take much longer to converge, which rationalizes our choice for a simpler reaction coordinate that is sufficient to resolve the large hysteresis observed in the FEP calculations. The simplest choice for this confinement coordinate is the distance between the COM of the α-amino group of the ligand and the COM of the two oxygens in the E705 side chain. This requires construction of a 1-D PMF, and therefore is computationally less costly than restraining the two dihedrals of E705, which would require construction of a 2-D PMF. For both the apo and the bound states, we use 14 windows between the distances 2.5 and 9.0 Å spaced 0.5 Å apart. Note that the restrained, noninteracting ligand is still present in the apo state though it has no effect on the protein. The chosen range is sufficient to cover all of the possible distances between these two groups as values outside this range are forbidden due to the limited flexibility of the E705 side-chain or steric clashes with the neighboring groups. The initial windows for umbrella sampling simulations are created from 2 ns of steered MD. A spring constant of 8 (kcal/mol)/Å^2 is employed, and each umbrella window is equilibrated for 2 ns followed by 3 ns of data production.

Model System and Simulation Details. The simulation systems are prepared using the crystal structures of GluA2 S1S2 ligand binding domain in complex with five ligands, namely, glutamate (Protein Data Bank (PDB) ID: 1FTJ), AMPA (1FTM), ACPA (1M5E), CNQX (3B7D), DNQX (1FTL), and the apo state of GluA2 (1FTO). The structures of the five ligands are shown in Figure 2. In all cases only one monomer (chain A) is used. All simulation boxes are created using the

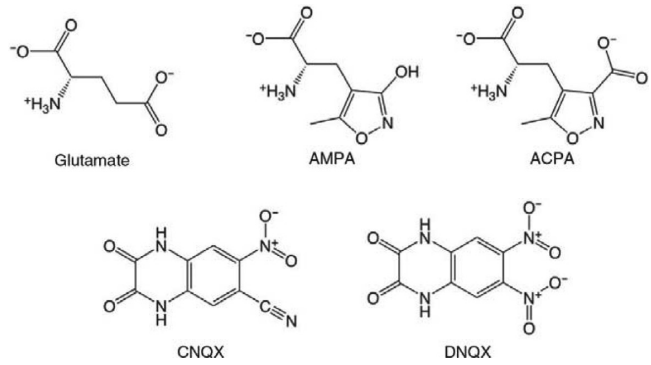

Figure 2. Structures of the five ligands considered in this study.

software VMD.[65] The apo protein or complex is solvated in a box of dimensions 80 × 80 × 70 Å^3 with about 12,000 water molecules. This size is chosen to ensure that, during the decoupling of the ligands in bulk, they do not interact with the protein (the ligands are more than 25 Å away from the binding site). To create a 0.15 M NaCl solution and maintain the charge neutrality, we add to the solution 34 Na^+ and 38 or 39 Cl^- ions, depending on the ligand bound. The total number of atoms in each system is about 40,000.

After energy minimization of each system, the restraints on the non-hydrogen atoms of the protein and ligand are gradually released during 5 ns of MD simulations. Each system is further simulated for 4 ns with no restraints applied. In order to compare our results to experimental values and to the PMF results,[44] we perform the FEP simulations in the same open state of the receptor as that employed in ref 44. This state is defined by introducing two distance restraints between groups of atoms in lobes S1 and S2, namely, ξ_1 which measures the distance between the COM of residues 479−481 in S1 and the COM of residues 654−655 in S2, and ξ_2 which measures the distance between the COM of residues 401−403 in S1 and the COM of residues 686−687 in S2. These distances are restrained at (ξ_1, ξ_2) = (14.4 Å, 13.7 Å). We perform 2 ns steered MD to achieve this state from the initial equilibrated complex, while keeping the ligands bound to the R485 residue on S1 and restraining the protein root-mean-square deviation (rmsd) separately on the S1 and S2 lobes, as

dx.doi.org/10.1021/jp412195m | J. Phys. Chem. B 2014, 118, 1813−1824

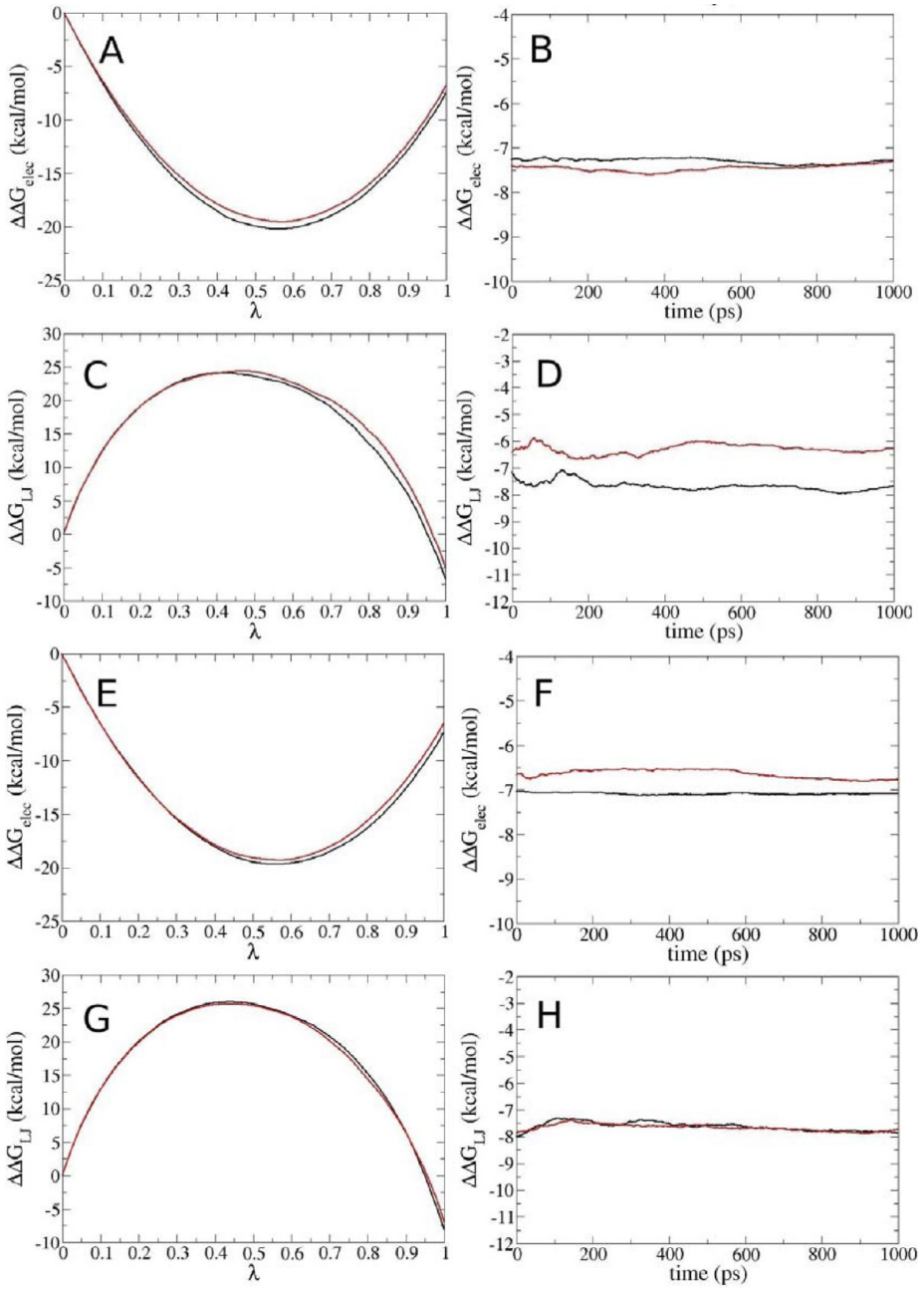

Figure 3. Plots of the FEP (first column) and TI (second column) calculations for the electrostatic (A, B) and LJ (C, D) interactions in CNQX, respectively. Graphs E–H show the same for DNQX. The black lines indicate the forward transformations, and the red lines, the negative of the backward transformations.

described in ref 44. After the steered MD is completed, we release the ligand and the rmsd restraints and simulate the resulting system for a further 5 ns. Throughout the following MD simulations and in all of the FEP calculations, restraints are applied to the ξ_1 and ξ_2 distances keeping them at (ξ_1, ξ_2) = (14.4 Å, 13.7 Å). In order to compare the values obtained for the ligand affinities in the open state to the experimental values, we add the free energy of LBD closure obtained from ref 44 to the final value of the binding free energy of each ligand.

All of our MD simulations are performed using the NAMD package (version 2.9)[66] with the CHARMM36 force field.[67] Initial parameters for ACPA, AMPA, CNQX, and DNQX were obtained from the ParamChem server,[5,6] and parameters with penalties higher than 10 were optimized using Gaussian 09.[7] The temperature is maintained at 300 K using Langevin damping with a coefficient of 5 ps^{-1}, and the pressure is kept at 1 atm using the Langevin piston method with a damping coefficient of 20 ps^{-1}.[68] Periodic boundary conditions with the particle-mesh Ewald method are employed to calculate the electrostatic interactions without truncation. The LJ interactions are switched off between 10 and 12 Å using a smooth switching function. A time step of 2 fs is used in all MD simulations.

RESULTS AND DISCUSSION

The results of the FEP/TI calculations are summarized in Table 1, and the standard binding free energies obtained are compared to those determined from umbrella sampling[44] and experiments.[53−55] The electrostatic and LJ contributions to the

dx.doi.org/10.1021/jp412195m | J. Phys. Chem. B 2014, 118, 1813−1824

Table 2. Comparison of the Entropic Contributions to the Free Energy Obtained with and without Restraints[a]

	CNQX	DNQX	ACPA	Glu	AMPA
$\Delta\Delta G_{rot}$	4.4	3.2*	4.5	3.9	4.6
$\Delta\Delta G_{rot\text{-}ent}$	4.0	3.6*	4.6	3.4	4.3
$\Delta\Delta G^0_{tr}$	3.8	3.6	4.1	3.8	4.0
$\Delta\Delta G^0_{tr\text{-}ent}$	3.4	3.4	3.9	3.6	4.0

[a]The free energy changes due to rotational and translational restraints from Table 1 are reproduced in rows 1 and 3. The free energy changes calculated from the rotational and translational entropies (eqs 9 and 10) are listed in rows 2 and 4 for comparison. All energies are in kcal/mol.

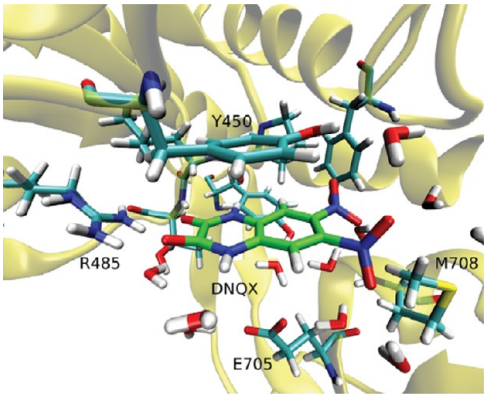

Figure 4. Snapshot of the DNQX complex in the open state of the receptor showing the hydrophobic interaction between the double ring of DNQX and the ring of the Y450 residue. The same pattern is also observed in the CNQX complex.

interaction free energy have been calculated using both the FEP and TI methods, and also in both the forward and backward directions to check for any hysteresis effects. The two methods yield very similar results; therefore only the TI results are shown in Table 1 as they allow for longer sampling and also estimation

Table 3. Restraint Dependence of the Translocation Free Energy[a]

restraints	$\Delta\Delta G_{elec}$	$\Delta\Delta G_{LJ}$	$\Delta\Delta G_{int}$
$k_t = 5$, $k_r = 300$	−7.2	−7.2	−14.4
$k_t = 10$, $k_r = 100$	−6.6	−7.6	−14.2
$k_t = 10$, $k_r = 300$	−7.1	−7.3	−14.4
$k_t = 10$, $k_r = 500$	−6.7	−8.0	−14.7
$k_t = 25$, $k_r = 300$	−6.4	−7.0	−13.4

[a]Results of the FEP calculations for the electrostatic and LJ terms and their sum for DNQX using different translational and orientational restraints for the ligand. The free energy is in kcal/mol, k_t is in (kcal/mol)/Å^2, and k_r is in (kcal/mol)/rad^2.

of the errors by block data analysis. As mentioned in Theory and Methods, all of the calculations are performed in the same open state of the receptor as in ref 44. This enables a direct comparison of the computational results obtained using the FEP/TI methods here with those determined from the PMF method. Also using the free energy of receptor closure from ref 44 allows us to determine the final standard binding free energy of the ligands, which can be compared with experiments. We first discuss CNQX and DNQX, which have similar structures and give very similar results, followed by discussions of the more challenging cases of ACPA, glutamate, and AMPA.

CNQX and DNQX. CNQX and DNQX are antagonists whose binding to the receptor prevents closure of the LBD. Consistent with these properties, both ligands have substantially larger affinities for the open state of the receptor compared to the agonists ACPA, glutamate, and AMPA (row 8 in Table 1), and much smaller free energies of closure (row 9). The main aim of this work is to demonstrate the feasibility of using the FEP/TI methods in calculation of the translocation free energies in ligand binding. To this end, we study the quality and convergence of the free energy calculations for the electrostatic and LJ terms. In Figure 3, we present the results of the FEP calculations as a function of the parameter λ, and the results of the TI calculations as running averages plotted as a function of the production time.

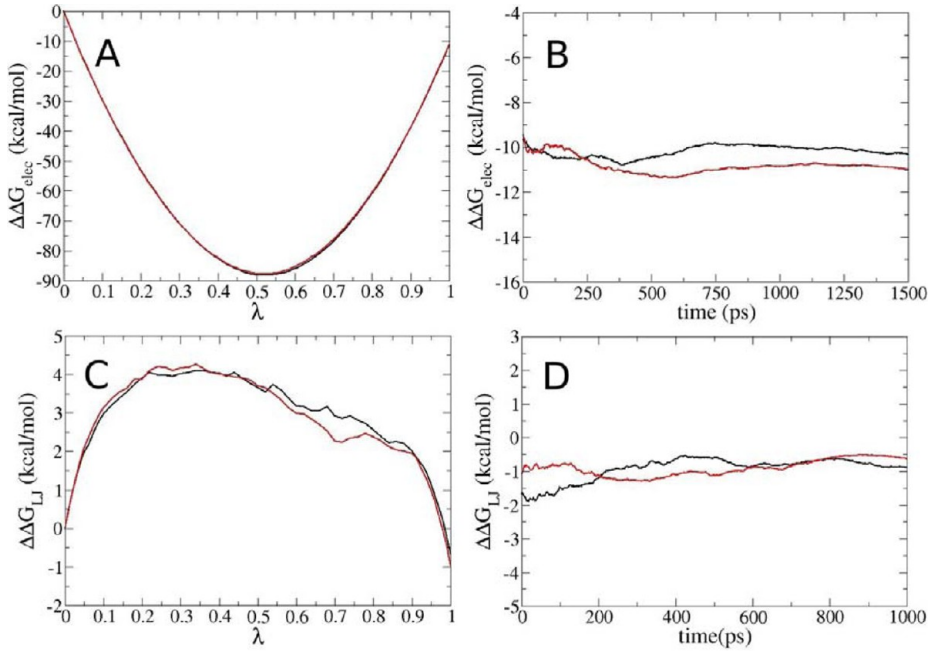

Figure 5. Same as Figure 3 but for ACPA. Plots of the FEP (first column) and TI (second column) calculations for the electrostatic (A, B) and LJ (C, D) interactions.

dx.doi.org/10.1021/jp412195m | J. Phys. Chem. B 2014, 118, 1813−1824

In both cases, the free energy difference $\Delta\Delta G$ is given by the endpoints in the plots. Comparison of the forward and backward transformation results shows that there is a minimal hysteresis effect in all cases. For example, in TI calculations the difference between the two sets is seen to be less than 1 kcal/mol in all cases except for $\Delta\Delta G_{LJ}$ in CNQX where it is 1.5 kcal/mol. Also the FEP and TI results obtained from the average of the forward and backward transformations are consistent with each other. Comparison of the standard binding free energies with those obtained from umbrella sampling and experiments (Table 1) provides further support for the feasibility of the FEP/TI approach—for both CNQX and DNQX, the calculated values are within 1 kcal/mol of the umbrella sampling and experimental results.

In Table 2, we compare the results of free energy changes calculated from the rotational and translational entropies of an unrestrained ligand using eqs 9 and 10 with those obtained from application of the rotational and translational restraints as presented in Table 1. The two methods are seen to yield very close results. In fact, using the values obtained from eqs 9 and 10 in Table 1, one would get very similar results for the binding free energies. The entropy calculations for an unrestrained ligand using eqs 9 and 10 are much easier and computationally less demanding than the free energy calculations involving application of rotational and translational restraints to a ligand. Therefore, it is worthwhile to check whether this alternative approach can be justified. Because restraints have to be used in calculation of the translocation free energy of a ligand in eq 2, we need to show that the force-field interactions of the ligand in the binding site/bulk are not affected by restraining its position and orientation. We test this conjecture by performing FEP calculations for the electrostatic and LJ parts of DNQX using different sets of restraints. The results shown in Table 3 are all very similar, indicating that, for reasonable choices, these restraints have indeed little effect on the force-field contributions to the binding free energy.

A distinguishing feature of the CNQX and DNQX results in Table 1 is the relatively large contribution of the LJ term to the binding free energy compared to the other ligands. This is directly responsible for the much higher affinities of CNQX and DNQX for the open state of the receptor, and therefore warrants a better understanding. The LJ term arises mostly from the hydrophobic interactions of the ligands with the receptor. Inspection of the binding modes of CNQX and DNQX shows that such an interaction occurs between the double ring of CNQX/DNQX and the ring of the Y450 residue of the receptor as shown in Figure 4. These two structures are observed to be stacked stably on top of each other during the entire MD simulations, suggesting that this interaction is a major contributor to the high affinity of these two antagonists in the open state of the receptor.

ACPA. ACPA differs from CNQX and DNQX in that it has a net charge $-e$ but lacks the double ring structure. These differences help to explain the stronger electrostatic and weaker LJ interactions in ACPA relative to CNQX and DNQX (Table 1). Quality and convergence of the FEP and TI calculations for the electrostatic and LJ terms are studied in Figure 5. In all cases, the forward and backward results differ by less than 1 kcal/mol, indicating a minimal hysteresis effect. Also there is an almost perfect agreement between the FEP and TI results. Yet the calculated standard binding free energy deviates from the experimental value by 1.7 kcal/mol—the only case among the five ligands where this deviation is larger than 1 kcal/mol. To see if this is due to some fluctuation, we have repeated the TI calculations but obtained essentially the same results. Another possibility is that the free energy of the receptor closure ΔG_{close} might be slightly overestimated, leading to the lower free energy value.

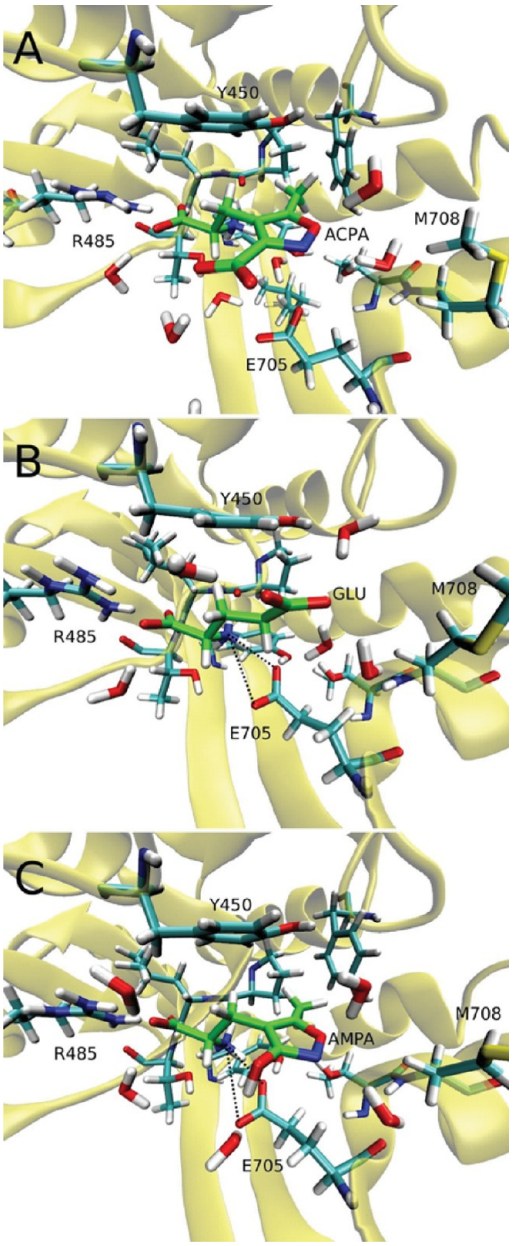

Figure 6. Snapshots of the ACPA, glutamate, and AMPA complexes in the open state of the receptor. The critical E705 side chain has no interactions with ACPA but makes salt bridges with the α-amino group of glutamate and AMPA (indicated by dotted lines).

Glutamate and AMPA. As mentioned in Theory and Methods, large hysteresis effects have been observed in the FEP calculations of the electrostatic terms for glutamate and AMPA. Despite its similarity with AMPA, this does not happen for ACPA. To explain why the hysteresis effect occurs for glutamate and AMPA and not for ACPA, we show snapshots of these ligands in complex with the open state of the receptor (Figure 6). It is seen that, in the case of glutamate and AMPA, there is a salt bridge between the ligand's α-amino group and the E705 side chain of the receptor, but this does not occur in ACPA. Thus the problem is caused by this salt bridge, and to circunvent it, we use

dx.doi.org/10.1021/jp412195m | J. Phys. Chem. B 2014, 118, 1813−1824

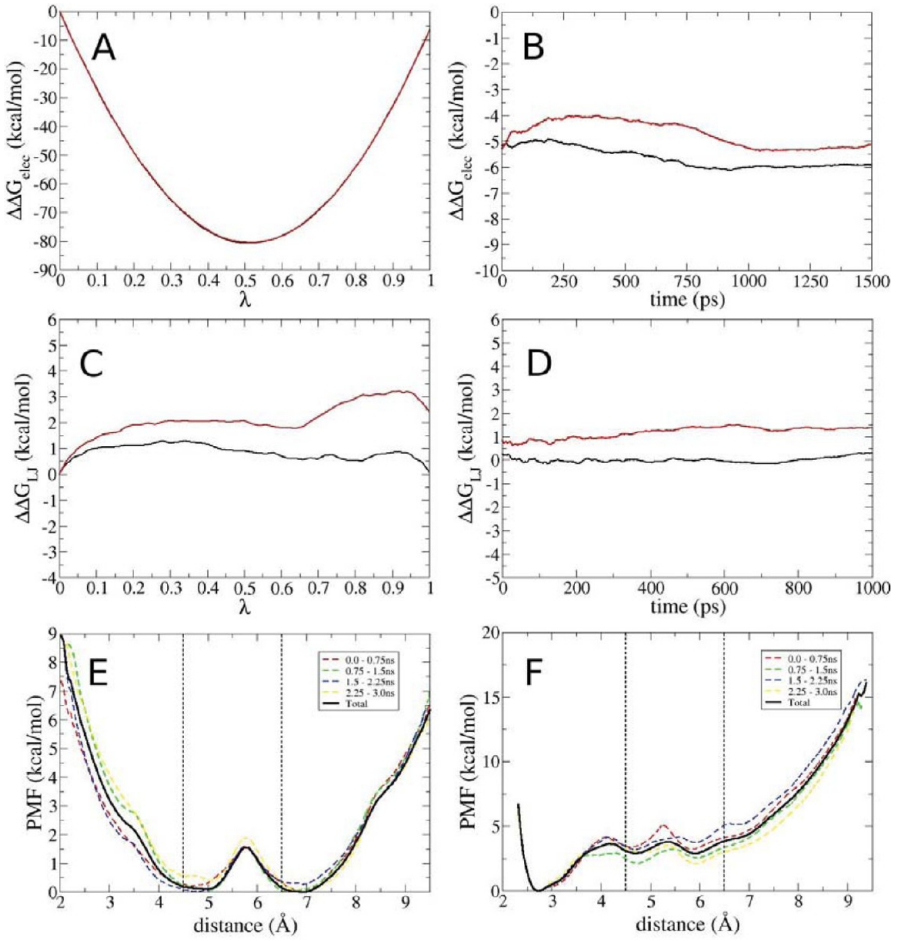

Figure 7. Plots of the FEP (first column) and TI (second column) calculations for the electrostatic (A, B) and LJ (C, D) interactions in glutamate. We also show the PMF as a function of the distance between the ligand α-amino and the receptor E705 side-chain carboxyl group in the apo (E) and bound (F) states of the receptor. The range of the confinement potential is indicated by the vertical dotted lines.

the confine-and-release method as outlined in Theory and Methods.

For glutamate, we confine the distance between the ligand α-amino and the receptor E705 side-chain carboxyl groups to the range of 4.5−6.5 Å by adding high energy barriers at these two points, which keeps the distance unbiased but confined within the specified range. This procedure breaks the salt bridge during the FEP simulations, and the contribution of this interaction is added later through the PMF term. The results of the FEP and TI calculations for the electrostatic and LJ terms, as well as the PMFs for the apo and bound states, are shown in Figure 7. Apart from the FEP result for the LJ term, there is minimal hysteresis between the forward and backward results. Because there is good agreement between the average FEP and TI results for the LJ term, we have not pursued this issue further. Convergence of the PMF results is demonstrated via block data analysis of the trajectory data (Figure 7E,F). The four PMF's constructed using 0.75 ns of data for each exhibit small fluctuations around the full PMF, which is taken as a sign of convergence. The standard binding free energy is in good agreement with the umbrella sampling and experimental results (Table 1), which shows that hysteresis problems in the FEP calculations can be overcome using the confine-and-release approach (Table 1). This is especially useful for calculations involving charged ligands because they often produce the largest conformational changes upon binding to a protein, and these changes can compromise the reliability of FEP calculations. By identifying the interactions causing problems and analyzing them separately, we can avoid such problems at the cost of some additional computations.

In the case of AMPA, using the same confinement range as in glutamate have still resulted in a large hysteresis in the FEP calculations. Therefore we have reduced the confinement range from 4.5−6.5 to 5.5−6.5 Å, further hindering the interaction between these two charged groups. As shown in Figure 8, this smaller range solved the hysteresis problem in the FEP calculations, yielding well-converged results in all FEP, TI, and PMF calculations. The standard binding free energy is within 1 kcal/mol of the experimental value but 1.5 kcal/mol smaller than the umbrella sampling result (Table 1). We note that this is the case among the five ligands where the difference between the FEP/TI and umbrella sampling results is largest. Another point to note is the relatively large contribution of the confine-and-release terms to the binding free energy of AMPA (rows 4 and 5 in Table 1). This is partly caused by the confinement potential which keeps the charged groups in the salt bridge further apart in AMPA compared to glutamate. Another reason can be gleaned from Figure 6. In the case of glutamate, there is some repulsive interaction between the β-carboxyl group and the E705 side-chain carboxyl, which reduces the effectiveness of the salt bridge. In AMPA, the carboxyl group is replaced by hydroxyl attached to the isoxazole ring, which does not hinder the formation of the salt bridge; rather it makes a hydrogen bond with E705. We can also

dx.doi.org/10.1021/jp412195m | J. Phys. Chem. B 2014, 118, 1813−1824

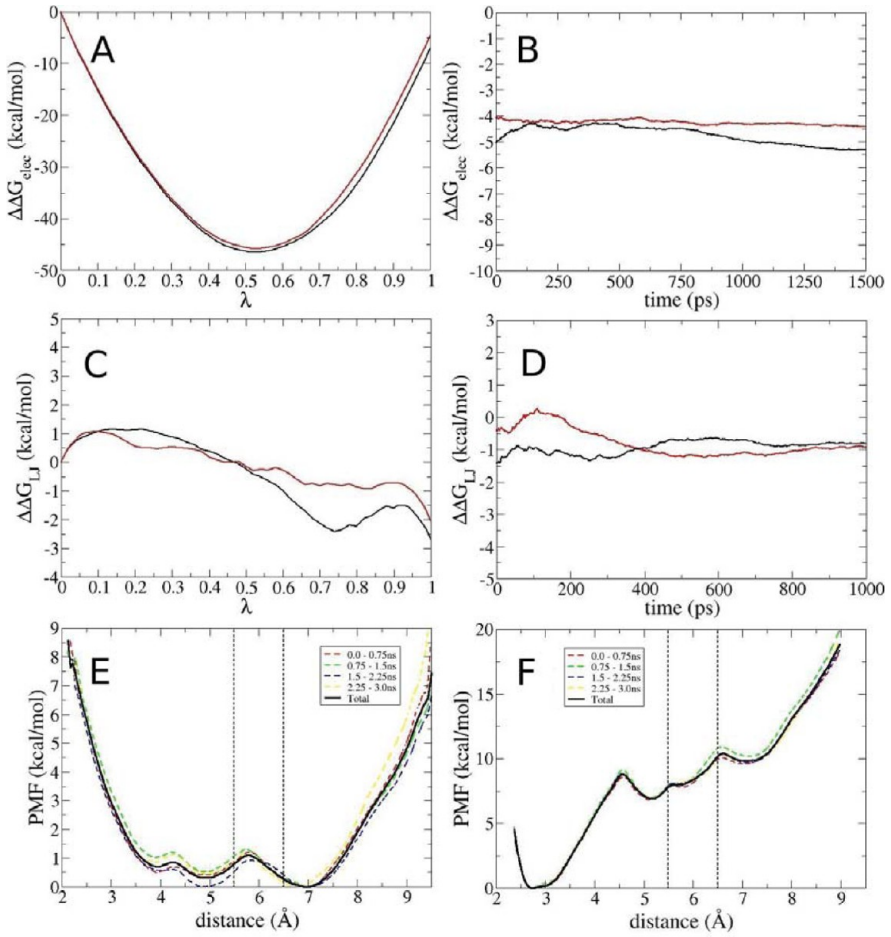

Figure 8. Same as Figure 7 but for AMPA. In this case, the range of the confinement potential is 5.5−6.5 Å.

see why the salt bridge does not form in ACPA—it is prevented by attachment of a carboxyl group instead of hydroxyl to the isoxazole ring. Thus the carboxyl group of E705 plays a critical role in binding of agonist ligands to the open state of GluA2.

CONCLUSION

In this study we have performed FEP/TI calculations of five polar and charged ligands using different techniques to obtain their standard binding free energies to the glutamate receptor GluA2. The FEP/TI calculations are performed by restraining the position and orientation of ligands using the absolute coordinates, which do not require anchoring atoms in the protein and ligand, and therefore are easier to implement. It also allows a direct calculation of the entropy differences between the free and bound states of the ligand. We have shown that this approach produces very similar results to the double decoupling method and, considering its simplicity, may offer an alternative method for the calculation of the standard binding free energies. For glutamate and AMPA, for which the straightforward FEP calculations lacked good convergence, we have used the confine-and-release method and obtained very good agreement with the experimental values. The results obtained in this study show that it is possible to calculate the binding free energies accurately using the FEP/TI methods even for ligands with net charges as long as the bulk and binding site transformations are performed in the same system. The FEP/TI methods, even though not suitable for protein−protein binding, are advantageous over the PMF method for binding sites that are deeply buried inside proteins. The techniques used here can be applied to many protein−ligand systems. The accuracy of the results means that they could, in particular, become very useful tools in rational drug design.

AUTHOR INFORMATION

Corresponding Author

*E-mail: serdar@physics.usyd.edu.au. Phone: ++61 2-9036-5306.

Notes

The authors declare no competing financial interest.

ACKNOWLEDGMENTS

This work was supported by grants from the Australian Research Council. Calculations were performed using the HPC facilities at the National Computational Infrastructure (Canberra) and the Victorian Life Sciences Computation Initiative (Melbourne).

REFERENCES

(1) Vindigni, A. Energetic Dissection of Specificity in Serine Proteases. *Comb. Chem. High Throughput Screening* **1999**, *2*, 139−153.

(2) Cheng, A. C.; Calabro, V.; Frankel, A. D. Design of RNA-Binding Proteins and Ligands. *Curr. Opin. Struct. Biol.* **2001**, *11*, 478−484.

(3) Mobley, D. L.; Klimovich, P. V. Perspective: Alchemical Free Energy Calculations for Drug Discovery. *J. Chem. Phys.* **2012**, *137*, 230901.

(4) Wang, J.; Wang, W.; Kollman, P. A.; Case, D. A. Automatic Atom Type and Bond Type Perception in Molecular Mechanical Calculations. *J. Mol. Graphics Modell.* **2006**, *25*, 247−260.

(5) Vanommeslaeghe, K.; MacKerell, A. D. Automation of the CHARMM General Force Field (CGenFF) I: Bond Perception and Atom Typing. *J. Chem. Inf. Model.* **2012**, *52*, 3144−3154.
(6) Vanommeslaeghe, K.; Raman, E. P.; MacKerell, A. D. Automation of the CHARMM General Force Field (CGenFF) II: Assignment of Bonded Parameters and Partial Atomic Charges. *J. Chem. Inf. Model.* **2012**, *52*, 3155−3168.
(7) Frisch, M. J.; Trucks, G. W.; Schlegel, H. B.; Scuseria, G. E.; Robb, M. A.; Cheeseman, J. R.; Scalmani, G.; Barone, V.; Mennucci, B.; Petersson, G. A.; et al. *Gaussian 09*, Revision D.01; Gaussian: Wallingford, CT, USA, 2009.
(8) Gohlke, H.; Klebe, K. Approaches to the Description and Prediction of the Binding Affinity of Small-Molecule Ligands to Macromolecular Receptors. *Angew. Chem., Int. Ed.* **2002**, *41*, 2644−2676.
(9) Warren, G. L.; Andrews, C. W.; Capelli, A. M.; Clarke, B.; LaLonde, J.; Lambert, M. H.; Lindvall, M.; Nevins, N.; Semis, S. F.; Senger, S.; et al. A Critical Assessment of Docking Programs and Scoring Functions. *J. Med. Chem.* **2006**, *49*, 5912−5931.
(10) Gilson, M. K.; Given, J. A.; Bush, B. L.; McCammon, J. A. The Statistical-Thermodynamic Basis for Computation of Binding Affinities: A Critical Review. *Biophys. J.* **1997**, *72*, 1047−1069.
(11) Boresch, S.; Tettinger, F.; Leitgeb, M.; Karplus, M. Absolute Binding Free Energies: A Quantitative Approach for Their Calculation. *J. Phys. Chem. B* **2003**, *107*, 9535−9551.
(12) Gilson, M. K.; Zhou, H. X. Calculation of Protein-Ligand Binding Energies. *Annu. Rev. Biophys. Biomol. Struct.* **2007**, *36*, 21−42.
(13) Deng, Y.; Roux, B. Computations of Standard Binding Free Energies with Molecular Dynamics Simulations. *J. Phys. Chem. B* **2009**, *113*, 2234−2246.
(14) Christ, C. D.; Mark, A. E.; van Gunsteren, W. F. Basic Ingredients of Free Energy Calculations. *J. Comput. Chem.* **2010**, *31*, 1569−1582.
(15) Chipot, C.; Pohorille, A. *Free Energy Calculations. Theory and Applications in Chemistry and Biology*; Springer Verlag: Berlin, 2007.
(16) Lelivre, T.; Rousset, M.; Stoltz, G. *Free Energy Computations: A Mathematical Perspective*; Imperial College Press: London, 2010.
(17) Chipot, C. Frontiers in Free-Energy Calculations of Biological Systems. *Wiley Interdiscip. Rev.: Comput. Mol. Sci.* **2013**, *4*, 71−89.
(18) Shirts, M. R.; Pitera, J. W.; Swope, W. C.; Pande, V. S. Extremely Precise Free Energy Calculations of Amino Acid Side Chain Analogs: Comparison of Common Molecular Mechanics Force Fields for Proteins. *J. Chem. Phys.* **2003**, *119*, 5740−5761.
(19) Deng, Y.; Roux, B. Hydration of Amino Acid Side Chains: Nonpolar and Electrostatic Contributions Calculated from Staged Molecular Dynamics Free Energy Simulations with Explicit Water Molecules. *J. Phys. Chem. B* **2004**, *108*, 16567−16576.
(20) Mann, G.; Hermans, J. Modeling Protein-Small Molecule Interactions: Structure and Thermodynamics of Noble Gases Binding in a Cavity in Mutant Phage T4 Lysozyme L99A. *J. Mol. Biol.* **2000**, *302*, 979−989.
(21) Fujitani, H.; Tanida, Y.; Ito, M.; Jayachandran, G.; Snow, C. D.; Shirts, M. R.; Sorin, E. J.; Pande, V. S. Direct Calculation of the Binding Free Energies of FKBP Ligands. *J. Chem. Phys.* **2005**, *123*, 084108.
(22) Oostenbrink, C.; van Gunsteren, W. F. Free Energies of Ligand Binding for Structurally Diverse Compounds. *Proc. Natl. Acad. Sci. U. S. A.* **2005**, *102*, 6750−6754.
(23) Mobley, D. L.; Chodera, J. D.; Dill, K. A. On the Use of Orientational Restraints and Symmetry Corrections in Alchemical Free Energy Calculations. *J. Chem. Phys.* **2006**, *125*, 084902.
(24) Deng, Y.; Roux, B. Calculation of Standard Binding Free Energies: Aromatic Molecules in the T4 Lysozyme L99A Mutant. *J. Chem. Theory Comput.* **2006**, *2*, 1255−1273.
(25) Wang, J.; Deng, Y.; Roux, B. Absolute Binding Free Energy Calculations Using Molecular Dynamics Simulations with Restraining Potentials. *Biophys. J.* **2006**, *91*, 2798−2814.
(26) Mobley, D.; Dumont, E.; Chodera, J.; Dill, K. Comparison of Charge Models for Fixed-Charge Force Fields: Small-Molecule Hydration Free Energies in Explicit Solvent. *J. Phys. Chem. B* **2007**, *111*, 2242−2254.
(27) Mobley, D. L.; Graves, A. P.; Chodera, J. D.; McReynolds, A. C.; Shoichet, B. K.; Dill, K. A. Predicting Absolute Ligand Binding Free Energies to a Simple Model Site. *J. Mol. Biol.* **2007**, *371*, 1118−1134.
(28) Karplus, M.; Kushick, J. N. Methods for Estimating the Configuratonal Entropy of Macromolecules. *Macromolecules* **1981**, *14*, 325−332.
(29) Hermans, J.; Wang, L. Inclusion of Loss of Translational and Rotational Freedom in Theoretical Estimates of Free Energies of Binding. Application to a Complex of Benzene and Mutant T4 Lysozyme. *J. Am. Chem. Soc.* **1997**, *119*, 2707−2714.
(30) Luo, H.; Sharp, K. On the Calculation of Absolute Macromolecular Binding Free Energies. *Proc. Natl. Acad. Sci. U. S. A.* **2002**, *99*, 10399−10404.
(31) Carlson, J.; Aqvist, J. Absolute and Relative Entropies from Computer Simulation with Applications to Ligand Binding. *J. Phys. Chem. B* **2005**, *109*, 6448−6456.
(32) Minh, D. D. L.; Bui, J. M.; Chang, C.; Jain, T.; Swanson, J. M. J.; McCammon, J. A. The Entropic Cost of Protein-Protein Association. *Biophys. J.* **2005**, *89*, L25−L27.
(33) Chang, C. A.; Chen, W.; Gilson, M. K. Ligand Configurational Entropy and Protein Binding. *Proc. Natl. Acad. Sci. U. S. A.* **2007**, *104*, 1534−1539.
(34) Gumbart, J. C.; Roux, B.; Chipot, C. Standard Binding Free Energies from Computer Simulations: What Is the Best Strategy? *J. Chem. Theory Comput.* **2013**, *9*, 794−802.
(35) Woo, H.; Roux, B. Calculation of Absolute Protein-Ligand Binding Free Energy from Computer Simulations. *Proc. Natl. Acad. Sci. U. S. A.* **2005**, *102*, 6825−6830.
(36) Bastug, T.; Chen, P. C.; Patra, S. M.; Kuyucak, S. Potential of Mean Force Calculations of Ligand Binding to Ion Channels from Jarzynski's Equality and Umbrella Sampling. *J. Chem. Phys.* **2008**, *128*, 155104.
(37) Chen, P. C.; Kuyucak, S. Mechanism and Energetics of Charybdotoxin Unbinding from a Potassium Channel from Molecular Dynamics Simulations. *Biophys. J.* **2009**, *96*, 2577−2588.
(38) Doudou, S.; Burton, N. A.; Henchman, R. H. Standard Free Energy of Binding form a One-Dimensional Potential of Mean Force. *J. Chem. Theory Comput.* **2009**, *5*, 909−918.
(39) Chen, P. C.; Kuyucak, S. Accurate Determination of the Binding Free Energy for KcsA-Charybdotoxin Complex from the Potential of Mean Force Calculations with Restraints. *Biophys. J.* **2011**, *100*, 2466−2474.
(40) Buch, I.; Sadiq, S. K.; De Fabritiis, G. Optimized Potential of Mean Force Calculations for Standard Binding Free Energies. *J. Chem. Theory Comput.* **2011**, *7*, 1765−1772.
(41) Chen, R.; Chung, S. H. Structural Basis of the Selective Block of Kv1.2 by Maurotoxin from Computer Simulations. *PLoS One* **2012**, *7*, No. e47253.
(42) Rashid, M. H.; Kuyucak, S. Affinity and Selectivity of ShK Toxin for the Kv1 Potassium Channels from Free Energy Simulations. *J. Phys. Chem. B* **2012**, *116*, 4812−4822.
(43) Gumbart, J. C.; Roux, B.; Chipot, C. Efficient Determination of Protein-Protein Standard Binding Free Energies from First Principles. *J. Chem. Theory Comput.* **2013**, *9*, 3789−3798.
(44) Lau, A. Y.; Roux, B. The Hidden Energetics of Ligand Binding and Activation in a Glutamate Receptor. *Nat. Struct. Mol. Biol.* **2011**, *18*, 283−287.
(45) Dixit, S. B; Chipot, C. Can Absolute Free Energies of Association Be Estimated from Molecular Mechanical Simulations? The Biotin−Streptavidin System Revisited. *J. Phys. Chem. A* **2001**, *105*, 9795−9799.
(46) Rocklin, G. J.; Boyce, S. E.; Fischer, M.; Fish, I.; Mobley, D. L.; Shoichet, B. K.; Dill, K. A. Blind Prediction of Charged Ligand Binding Affinities in a Model Binding Site. *J. Mol. Biol.* **2013**, *425*, 4569−4583.
(47) Heinzelmann, G.; Bastug, T.; Kuyucak, S. Free Energy Simulations of Ligand Binding to the Aspartate Transporter Glt_{Ph}. *Biophys. J.* **2011**, *101*, 2380−2388.
(48) Heinzelmann, G.; Bastug, T.; Kuyucak, S. Mechanism and Energetics of Ligand Release in the Aspartate Transporter Glt_{Ph}. *J. Phys. Chem. B* **2013**, *117*, 5486−5496.

(49) Rashid, M. H.; Heinzelmann, G.; Huq, R.; Tajhya, R. B.; Chang, S. C.; Chhabra, S.; Pennington, M. W.; Beeton, C.; Norton, R. S.; Kuyucak, S. A Potent and Selective Peptide Blocker of the Kv1.3 Channel: Prediction from Free-Energy Simulations and Experimental Confirmation. *PLoS One* **2013**, *8*, No. e78712.
(50) Hayashi, T. Effects of Sodium Glutamate on the Nervous System. *Keio J. Med.* **1954**, *3*, 183−192.
(51) Brauner-Osborne, H.; Egebjerg, J.; Nielsen, E. O.; Madsen, U.; Krogsgaard-Larsen, P. Ligands for Glutamate Receptors: Design and Therapeutic Prospects. *J. Med. Chem.* **2000**, *43*, 2609−2645.
(52) O'Neill, M. J.; Witkin, J. M. AMPA Receptor Potentiators: Application for Depression and Parkinson's Disease. *Curr. Drug Targets* **2007**, *8*, 603−620.
(53) Ahmed, A. H.; Thompson, M. D.; Fenwick, M. K.; Romero, B.; Loh, A. P.; Jane, D. E.; Sondermann, H.; Oswald, R. E. Mechanisms of Antagonism of the GluR2 AMPA Receptor: Structure and Dynamics of the Complex of Two Willardiine Antagonists with the Glutamate Binding Domain. *Biochemistry* **2009**, *48*, 3894−3903.
(54) Armstrong, N.; Gouaux, E. Mechanisms for Activation and Antagonism of an AMPA-Sensitive Glutamate Receptor: Crystal Structures of the GluR2 Ligand Binding Core. *Neuron* **2000**, *28*, 165−181.
(55) Hogner, A.; Kastrup, J. S.; Jin, R.; Liljefors, T.; Mayer, M. L.; Egebjerg, J.; Larsen, I. K.; Gouaux, E. Structural Basis for AMPA Receptor Activation and Ligand Selectivity: Crystal Structures of Five Agonist Complexes with the GluR2 Ligand-Binding Core. *J. Mol. Biol.* **2002**, *322*, 93−109.
(56) Menuz, K.; Stroud, R. M.; Nicoll, R. A.; Hays, F. A. TARP Auxiliary Subunits Switch AMPA Receptor Antagonists into Partial Agonists. *Science* **2007**, *318*, 815−817.
(57) Wolter, T.; Steinbrecher, T.; Elstner, M. Computational Study of Synthetic Agonist Ligands of Ionotropic Glutamate Receptors. *PLoS One* **2013**, *8*, No. e58774.
(58) Jo, S.; Jiang, W.; Lee, H. S.; Roux, B.; Im, W. CHARMM-GUI Ligand Binder for Absolute Binding Free Energy Calculations and Its Application. *J. Chem. Inf. Model.* **2012**, *53*, 267−277.
(59) Zacharias, M.; Straatsma, T. P.; McCammon, J. A. Separation-Shifted Scaling, a New Scaling Method for Lennard-Jones Interactions in Thermodynamic Integration. *J. Chem. Phys.* **1994**, *100*, 9025−9031.
(60) Kofke, D. A.; Cummings, P. T. Precision and Accuracy of Staged Free-Energy Perturbation Methods for Computing the Chemical Potential by Molecular Simulation. *Fluid Phase Equilib.* **1998**, *150*, 41−49.
(61) Bennett, C. H. Efficient Estimation of Free Energy Differences from Monte Carlo Data. *J. Comput. Phys.* **1976**, *22*, 245−268.
(62) Pohorille, A.; Jarzynski, C.; Chipot, C. Good Practices in Free-Energy Calculations. *J. Phys. Chem. B* **2010**, *114*, 10235−10253.
(63) Mobley, D. L.; Chodera, J. D.; Dill, K. A. Confine-and-Release Method: Obtaining Correct Binding Free Energies in the Presence of Protein Conformational Change. *J. Chem. Theory Comput.* **2007**, *3*, 1231−1235.
(64) Kumar, S. J.; Rosenberg, M.; Bouzida, D.; Swendsen, R. H.; Kollman, P. A. The Weighted Histogram Analaysis Method for Free-Energy Calculations on Biomolecules. I. The Method. *J. Comput. Chem.* **1992**, *13*, 1011−1021.
(65) Humphrey, W.; Dalke, A.; Schulten, K. VMD—Visual Molecular Dynamics. *J. Mol. Graphics* **1996**, *14*, 33−38.
(66) Phillips, J. C.; Braun, R.; Wang, W.; Gumbart, J.; Tajkhorshid, E.; Villa, E.; Chipot, C.; Skeel, R. D.; Kale, L.; Schulten, K. Scalable Molecular Dynamics with NAMD. *J. Comput. Chem.* **2005**, *26*, 1781−1802.
(67) Vanommeslaeghe, K.; Hatcher, E.; Acharya, C.; Kundu, S.; Zhong, S.; Shim, J.; Darian, E.; Guvench, O.; Lopes, P.; Vorobyov, I.; et al. CHARMM General Force Field: A Force Field for Drug-Like Molecules Compatible with the CHARMM All-Atom Additive Biological Force Field. *J. Comput. Chem.* **2010**, *31*, 671−690.
(68) Feller, S.; Zhang, Y.; Pastor, R.; Brooks, B. Constant Pressure Molecular Dynamics: The Langevin Piston Method. *J. Chem. Phys.* **1995**, *103*, 4613−4621.